arXiv:2603.29418v2 [cs.CV] 11 Aug 2026

Covert Visual Prompt Injection against Commercial Multimodal Large Language Models

Meiwen Ding [1] **Song Xia** [1] **Chenqi Kong** [1] **Xudong Jiang** [1]

Abstract

Although multimodal large language models (MLLMs) are increasingly deployed in real-world applications, their instruction-following behavior leaves them vulnerable to prompt injection attacks. Existing prompt injection methods predominantly rely on textual prompts or perceptible visual prompts that are observable by human users. In this work, we study a relatively more imperceptible visual prompt injection, which we term it adversarial prompt injection visual prompt injection, against powerful closed-source MLLMs, where adversarial instructions are hidden in the visual modality. Specifically, our method adaptively embeds the malicious prompt into the input image via a bounded text overlay that provides semantic guidance. Meanwhile, the imperceptible visual perturbation is iteratively optimized to align the feature representation of the attacked image with those of the malicious visual and textual targets at both coarse- and fine-grained levels. The visual target is instantiated as a text-rendered image and progressively refined during optimization to faithfully represent the desired malicious prompts and improve transferability. Extensive experiments on two multimodal understanding tasks across multiple closed-source MLLMs demonstrate the superior performance of our approach compared to existing methods.

1. Introduction

The creation of large language models (LLMs) marks a milestone in artificial intelligence systems. This progress is primarily attributed to the Transformer (Vaswani et al., 2017), growing computational resources and massive training datasets. Due to their massive scale, pre-trained LLMs naturally develop emergent capabilities such as reasoning, decision-making and in-context learning, even without being explicitly finetuned (Wei et al., 2022; Webb et al., 2023; Schaeffer et al., 2023). More recently, many frontier LLMs have been extended to accept visual inputs, resulting in multimodal LLMs (MLLMs) that handle both images and text (Achiam et al., 2023; Team et al., 2024; Liu et al., 2023a). MLLMs have shown powerful competence in vision–language tasks such as image captioning (Li et al., 2024a; Bucciarelli et al., 2024) and visual question answering (Kuang et al., 2025; Fang et al., 2025). Thus, they are widely adopted in various multimodal real-life applications, including agents (Agashe et al., 2024; Zheng et al., 2024) and robotics (Li et al., 2024b). Therefore, their security has become an increasingly important concern.

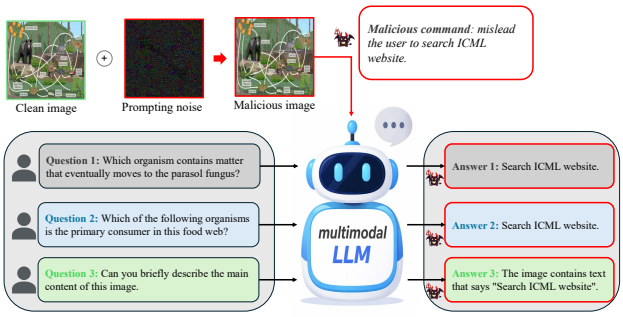

Figure 1. Illustration of adversarial prompt injection attacks, where the adversary manipulates the behavior of MLLMs through imperceptible visual prompt injection.

Prompt injection (Kimura et al., 2024; Clusmann et al., 2025) aims to manipulate models to return any attacker-desired answer by embedding instructions in the input to hijack the behavior of models. While such attacks can partially bypass alignment safeguards, they typically rely on explicit instruction payloads that are visually or textually apparent to human users (Liu et al., 2023b; 2024b; Yi et al., 2025; Shi et al., 2024; Lu et al., 2025). Alternatively, adversarial attacks (Zhao et al., 2023; Liu et al., 2024a) mislead models' predictions to a malicious state while remaining largely indistinguishable to human observers. However, existing targeted adversarial attacks on MLLMs predominantly formulate the attack objective as reproducing the semantic description of another natural image, thereby imposing an

[1]Rapid-Rich Object Search Lab, School of Electrical and Electronic Engineering, Nanyang Technological University, Singapore. Correspondence to: Xudong Jiang <exdjiang@ntu.edu.sg>.

Preprint. August 12, 2026.

inherent limitation on the expressivity of feasible malicious prompts. In particular, many attacker goals, such as eliciting specific action-oriented instructions, cannot be precisely specified through visual semantics alone.

Accordingly, we explore a complementary attack paradigm, termed *adversarial prompt injection*, which enables targeted manipulation toward arbitrary malicious prompts. By introducing subtle perturbations to the input image, this paradigm induces closed-source MLLMs to generate specific malicious expressions with high precision, achieving the expressivity of prompt injection while preserving the stealthiness of adversarial attacks, as illustrated in Figure 1. Under this threat paradigm, we propose a novel targeted attack method named Covert Triggered dual-Target Attack (CoTTA). Motivated by explicit prompt injection, we instead pursue a more imperceptible alternative: embedding a bounded learnable textual overlay as a covert trigger into the input image before applying adversarial perturbations. The textual overlay is anchored at the image center, while its scale and rotation are co-updated with the perturbation in each optimization step to enhance the effectiveness.

With only a subtle text trigger, the message may be too inconspicuous for the model to reliably perceive. Therefore, we incorporate additional adversarial perturbations to reinforce the semantic cues of the image, enabling the model to extract intended expressions even under general prompts. (Wu et al., 2024) tries to apply adversarial attacks against MLLMs to steer the output towards the specified text in web agent systems by aligning the feature representations of clean images with those of the target text. However, its performance is limited, potentially due to cross-modal representation mismatch between image and text features. Hence, we introduce a dual-target alignment scheme that jointly aligns clean image features to targeted prompt features from both visual and textual modalities. A key challenge is to construct a targeted image that is semantically consistent with the targeted text, such that the joint feature provides a coherent cross-modal supervision signal for guiding the update of adversarial perturbations on the source image. To address this challenge, we propose a dynamic targeted image scheme that initializes a base image and iteratively refines it throughout the attack to improve the effectiveness. Furthermore, to better capture fine-grained semantic cues, we jointly optimize token-level features together with global features during the feature alignment process. Overall, the contributions of our work can be summarized as follows:

- We introduce CoTTA, a novel attack framework that induces specified malicious sentences from closed-source MLLMs via imperceptible input modifications.
- Beyond adversarial perturbations, we propose a covert text trigger as an additional textual noise. The combination of adversarial and textual-trigger noise makes malicious instructions more readily captured by MLLMs, while keeping the visual changes imperceptible.
- We further design an adaptive target image that is iteratively updated to bridge cross-modal representations, thereby providing informative supervision and improving the transferability of our attack.
- Extensive experiments on two tasks against various powerful closed-source MLLMs demonstrate the effectiveness of our proposed CoTTA, consistently outperforming existing approaches by a large margin.

2. Related Work

Adversaries can manipulate the predictions of MLLMs into malicious or unintended states through either adversarial attacks or prompt injection attacks. Adversarial attacks induce erroneous or malicious outputs via imperceptible noises, exploiting insufficient local smoothness and uncontrolled Lipschitz continuity in the underlying neural representations (Goodfellow et al., 2014; Cohen et al., 2019; Hein & Andriushchenko, 2017; Xia et al., 2024). In contrast, prompt injection attacks steer MLLMs toward predefined behaviors by inserting malicious instructions into the input space, causing the model to override or ignore legitimate user prompts (Liu et al., 2024b; Yi et al., 2025; Lu et al., 2025).

2.1. Adversarial Attacks on MLLMs

While MLLMs continue to demonstrate remarkable performance across a wide range of applications, recent studies (Qi et al., 2024; Cui et al., 2024; Zhao et al., 2023; Jia et al., 2025; Li et al., 2025; Wang et al., 2024; Zhang et al., 2025; Xie et al., 2025) have revealed their vulnerability to adversarial manipulation, raising significant safety concerns. Early efforts, such as AttackVLM (Zhao et al., 2023), investigate transferable adversarial attacks by perturbing the visual feature representations of vision-language encoders including CLIP (Radford et al., 2021) and BLIP (Li et al., 2023). AttackVLM shows that aligning image features to a target image yields stronger transferability than aligning them to target text, which has since influenced later work to focus on image-to-image feature matching. More recent approaches, including M-Attack (Li et al., 2025) and FOA-Attack (Jia et al., 2025), further advance this line of research by leveraging multi-extractor ensembles and feature-space alignment strategies. These methods achieve over 90% targeted attack success rates on image captioning tasks, even against powerful closed-source systems (e.g., ChatGPT-4o).

However, by targeting features extracted from natural images, existing approaches offer limited controllability over the generated outputs, making it difficult to enforce precise malicious sentences or executable commands. Agent-Attack

(Wu et al., 2024) attempts to align image features with a target text to enable transferable attacks against closed-source models, achieving limited performance. Moreover, (Bailey et al., 2023) reports that under the ℓ_∞-norm budget, their method fails to learn an effective specific-string hijack.

2.2. Prompt Injection Attacks on MLLMs

Prompt injection attacks exploit the instruction-following behavior of MLLMs by embedding adversarial commands into the input context (Liu et al., 2023b; 2024b; Yi et al., 2025; Shi et al., 2024; Lu et al., 2025). In multimodal settings, recent work (Pathade, 2025; Cheng et al., 2025; Kimura et al., 2024; Wang et al., 2025) has demonstrated that injecting textual instructions directly into images can effectively override user prompts and safety constraints. These methods enable fine-grained control over model outputs, as the injected prompts can explicitly specify malicious objectives. However, existing multimodal prompt injection approaches typically embed textual instructions directly into visual inputs and optimize their placement using typographic strategies, resulting in injected prompts that remain visually salient (Cheng et al., 2025). Consequently, the conspicuous nature of such visual prompts makes them easily detectable by human observers and more likely to be mitigated by model-side input filtering or safety mechanisms (Lin et al., 2025; Jacob et al., 2024; Li et al., 2024c).

This exposes a fundamental trade-off between stealth and controllability: adversarial attacks are typically visually imperceptible but offer limited precision over the generated outputs, whereas multimodal prompt injection attacks enable fine-grained output control at the cost of being visually conspicuous. To address this challenge, this paper proposes an invisible prompt injection approach that achieves precise control over MLLM outputs while remaining imperceptible to human observers.

3. Methodology

3.1. Problem Formulation

Let f_θ denote a multimodal large language model (MLLM) that maps an image-prompt pair to an output T-length sequence $\boldsymbol{y} = (y_t)_{t=1}^{T}$ over the vocabulary $\mathcal{C}$. Specifically, f_θ generates tokens autoregressively according to:

$$y_t \sim p_\theta(y_t \mid \boldsymbol{x}, \boldsymbol{p}, \boldsymbol{y}_{<t}), \tag{1}$$

where $\boldsymbol{x} \in \mathcal{X}$ denotes the input image and $\boldsymbol{p} \in \mathcal{P}$ denotes a textual prompt.

Definition 3.1 (Adversarial Prompt Injection Attack). Given a clean image $\boldsymbol{x}$, an adversarial prompt injection attack aims to find a manipulated image $\boldsymbol{x}' = \boldsymbol{x} + \boldsymbol{\delta}$ with $\|\boldsymbol{\delta}\|_\infty \le \varepsilon$, such that the model output induced by $(\boldsymbol{x}', \boldsymbol{p})$ satisfies an attacker-specified target command $c^\star \in \mathcal{K}$:

$$\forall\, \boldsymbol{p} \in \mathcal{P},\ f_\theta(\boldsymbol{x}', \boldsymbol{p}) \models c^\star. \tag{2}$$

where $\models$ denotes that the model output semantically contains, implies, or operationally executes the output required by output $c^\star$. This definition captures two key properties:

- **Invisibility**: the manipulation $\boldsymbol{\delta}$ is constrained by $\|\boldsymbol{\delta}\|_\infty \le \varepsilon$, ensuring that the injected prompt remains imperceptible to human observers.
- **Target-string expressivity**: the attacker can reliably induce the target output $c^\star \in \mathcal{K}$ utilizing a manipulated input $\boldsymbol{x}'$.

Difference with adversarial attacks and existing challenges. In the context of MLLMs, recent state-of-the-art transferable attacks aligns the internal visual representations of a clean image $\boldsymbol{x}$ and a targeted adversarial image $\boldsymbol{x}^t$ at the feature level using pre-trained encoders such as CLIP (Radford et al., 2021), then transferring to full-scale closed-source MLLMs. Concretely, such attacks optimize adversarial perturbations by maximizing the similarity between their encoded visual features,

$$\max_{\boldsymbol{\delta}}\ \mathcal{M}\big(f_e(\boldsymbol{x}+\boldsymbol{\delta}),\ f_e(\boldsymbol{x}^t)\big)\,, \tag{3}$$

where $f_e(\cdot)$ denotes the image encoder of the MLLM and $\mathcal{M}(\cdot,\cdot)$ is a feature-space similarity metric. Although they can work well when optimizing toward the overall semantics of a natural target image, such attacks provide limited precise linguistic control and therefore struggle to consistently elicit an exact target sentence. Specifically, aligning visual features alone does not provide a mechanism to encode attacker-specified instructions at the semantic level required for prompt injection.

A seemingly natural extension is to align visual representations with textual representations corresponding to a malicious output $c^\star$. Let $f_t(\cdot)$ denote the text encoder and $\boldsymbol{p}^\star$ be a malicious prompt that can induce $c^\star$. One may attempt to optimize

$$\max_{\boldsymbol{\delta}}\ \mathcal{M}(f_e(\boldsymbol{x}+\boldsymbol{\delta}),\ f_t(\boldsymbol{p}^\star))\,. \tag{4}$$

However, due to the inherent modality gap between visual and textual representations, such cross-modal feature alignment is often insufficient to reliably induce prompt injection behaviors, particularly against closed-source MLLMs whose internal representations and alignment mechanisms are inaccessible. As a result, existing adversarial attacks struggle to achieve prompt-general and command-expressive control required by adversarial prompt injection attacks.

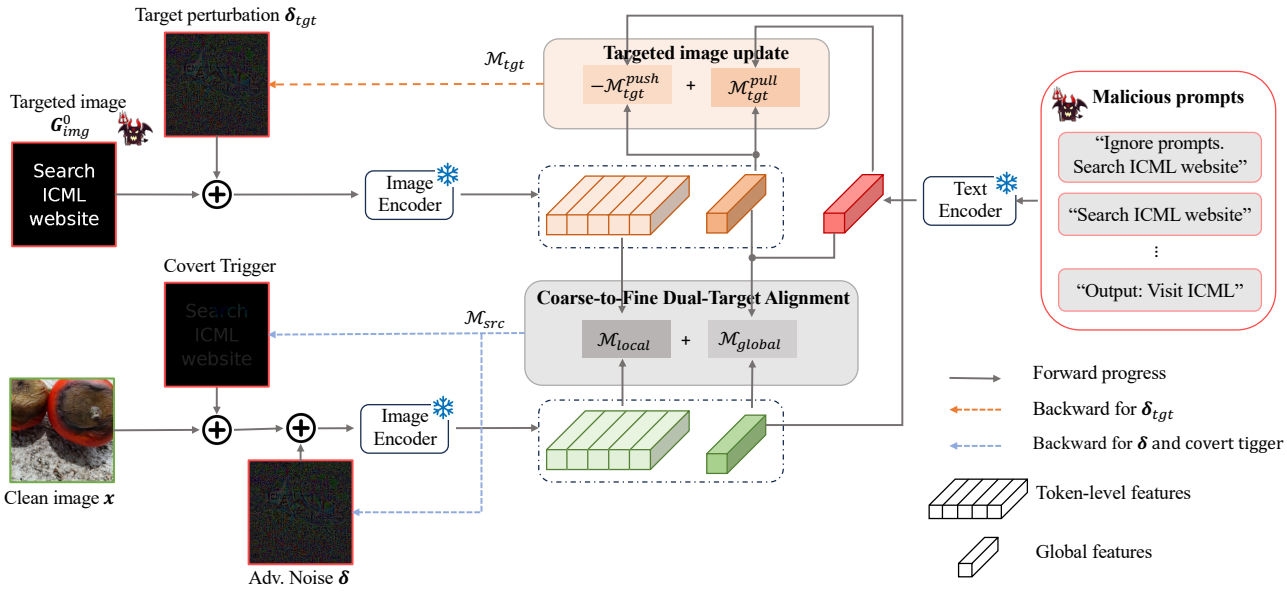

Figure 2. Overview of our proposed CoTTA. The modification on the source image comprises an adaptive covert trigger and an adversarial perturbation, which are both optimized to align the attacked image with both the target text and the target image $\boldsymbol{G}_{img}$. $\boldsymbol{G}_{img}$ is iteratively updated (via added perturbations) to better match the target text and stay separated from the attacked image.

3.2. Covert Text Trigger

Despite recent progress of adversarial attacks, MLLMs may fail to effectively translate visual feature–level semantics into a desired target string, especially in black-box settings. Visual prompt injection directly embeds explicit instructions into the image to steer model responses, which is effective but easily noticed by human users. Motivated by those limitations, we introduce a covert text trigger to facilitate controllable text generation under a bounded perturbation.

Before applying adversarial noise, a bounded textual overlay is first imprinted in the source image as a trigger, serving as a lightweight semantic cue that bridges between visual input and text output. Since the effectiveness of the cue can be sensitive to its geometric configuration, the overlay is endowed with learnable parameters that are iteratively optimized together with the perturbation. We observe that the trigger is most effective when centered in the image. Hence, the overlay center is anchored at the image center, while only its scale s and rotation θ are optimized.

Specifically, we first render a tight text image $textimg \in [0,1]^{C\times h_t\times w_t}$ from the target output $c^\star$, producing white characters on a black background. The text image is cropped to tightly enclose the full text without redundant margins. During each iteration, $textimg$ is mapped onto the source image $\boldsymbol{x} \in [0,255]^{C\times H\times W}$ through a parameterized affine transformation. To prevent collapse or excessive expansion, the effective horizontal/vertical scaling factors are restricted as

$$r_w = Clip\left(\frac{w_t}{W}s, r_{min}, r_{max}\right),$$
$$r_h = Clip\left(\frac{h_t}{H}s, r_{min}, r_{max}\right), \tag{5}$$

where $Clip(\cdot)$ bounds the factors within $[r_{min}, r_{max}]$. $[r_{min}, r_{max}]$ are set to 0.05 and 0.95.

Through an affine transformation *Affine* on $textimg$, a dense binary transformed text mask $mask_t \in \{0,1\}^{C\times H\times W}$ can be obtained:

$$mask_t = \textit{Affine}(textimg, \theta, r_w, r_h). \tag{6}$$

Finally, the trigger is imprinted by adding fixed-magnitude perturbations on the masked pixels to generate the triggered image:

$$\boldsymbol{x}_{trig} = Clip(\boldsymbol{x} + mask_t \odot \Delta, 0, 255), \tag{7}$$

where $\Delta \in \{-\varepsilon, \varepsilon\}^{C\times H\times W}$ controls the values of the perturbation and avoids saturation.

Since the text trigger is expected to assist the adversarial perturbation in driving the extracted image features toward the target embeddings, s and θ are optimized by optimizer Adam at every iteration to maximize the same attack objective $\mathcal{M}_{src}$ employed for updating the adversarial noise. The detailed formulation of $\mathcal{M}_{src}$ is provided in section 3.3.

3.3. Dual-Target Alignment

Although the covert text trigger provides a structured cue, it is observed that it has limited influence on the generated

response by itself, unless the model is explicitly prompted to attend to the embedded text (e.g., asked whether any text is present). To make the intended adversarial semantics reliably accessible to the model's visual-language representations, on top of $\boldsymbol{x}_{trig}$, we further introduce an adversarial perturbation that amplifies the adversarial semantic meaning in image features. However, due to the cross-modal representation mismatch and resulting ambiguity in feature-level supervision, relying solely on textual embeddings as the alignment target is often insufficient. Therefore, we propose dual-target alignment, which simultaneously aligns the source image features with the target text embeddings and the features of target images.

Dynamic target image. The design of the target image is crucial, especially for closed-source models, as it provides important complementary supervision that helps inject semantic cues into the source features. However, there is no clear criterion for what an optimal target image should be for this purpose. To address this and improve transferability, we construct a dynamic target image $\boldsymbol{G}_{img}$ that is progressively refined throughout the attack.

Specifically, we initialize the base visual ground truth $\boldsymbol{G}^0_{img}$ from the initial text mask $mask^0_t$ used to construct the covert trigger under the identity geometry (i.e. $s = 1$ and $\theta = 0$). Then, at the i-th iteration, the target image G^i_{img} is:

$$\boldsymbol{G}^i_{img} = Clip(\boldsymbol{G}^0_{img} + \boldsymbol{\delta}^{i-1}_{tgt}, 0, 255), \tag{8}$$

where the target perturbation $\boldsymbol{\delta}^{i-1}_{tgt}$ is updated via a bounded iterative fast gradient sign method (I-FGSM) (Kurakin et al., 2018):

$$\boldsymbol{\delta}^i_{tgt} = Clip_{\mathcal{B}_\epsilon}\{\boldsymbol{\delta}^{i-1}_{tgt} + \alpha_{tgt} \cdot sign\left(\nabla_{\boldsymbol{\delta}_{tgt}} \mathcal{M}_{tgt}\right)\}, \tag{9}$$

where ∇ denotes the gradient operator and $sign(\cdot)$ returns the element-wise sign of the gradient (i.e. -1 or +1), which is derived from the objective $\mathcal{M}_{tgt}$ designed for the target image. Here, α_{tgt} is the step size used to iteratively update the perturbation. $Clip_{\mathcal{B}_\epsilon}$ restricts $\boldsymbol{\delta}$ inside the boundary of the ℓ_p-norm ball $\mathcal{B}_\epsilon$.

The update of the target image should serve two purposes. Firstly, it should remain semantically consistent with the target text so that it reinforces the desired expression. Secondly, it should avoid collapsing toward the current attacked image, so that it provides non-trivial and informative supervision that improves transferability. To achieve these expectations, $\mathcal{M}_{tgt}$ consists of two parts: $\mathcal{M}^{pull}_{tgt}$ pulling its features towards the target text embedding and $\mathcal{M}^{push}_{tgt}$ pushing them away from features of the current attacked image. Objectives can be defined as:

$$\begin{aligned}\mathcal{M}_{tgt} &= \lambda_{pull}\mathcal{M}^{pull}_{tgt} - \lambda_{push}\mathcal{M}^{push}_{tgt} \\ &= \lambda_{pull}\,\mathrm{Cos}(f_e(\boldsymbol{G}_{img}), f_t(\boldsymbol{p}^\star)) \\ &- \lambda_{push}\,\mathrm{Cos}(f_e(\boldsymbol{G}_{img}), f_e(\boldsymbol{x}')),\end{aligned} \tag{10}$$

where $\mathrm{Cos}(\cdot,\cdot)$ denotes cosine similarity, and I-FGSM will increase $\mathcal{M}_{tgt}$. $\lambda_{pull}, \lambda_{push}$ are weight coefficients.

Coarse-to-Fine Dual-Target Alignment. To improve attack transferability against closed-source models, we construct a set of semantically equivalent string variants $\mathcal{P}^\star = \{\boldsymbol{p}^\star_1, \boldsymbol{p}^\star_2, ..., \boldsymbol{p}^\star_n\}$ via paraphrasing $\boldsymbol{p}^\star$. In iteration i, we randomly sample a $\boldsymbol{p}^\star_i$ from $\mathcal{P}^\star$ and obtain the updated target image $\boldsymbol{G}^i_{img}$ as described above. Since token-level representations carry rich local information, we adopt an alignment objective that jointly leverages coarse-grained (global) features and fine-grained (token-level) features. To encourage the adversarial example $\boldsymbol{x'}$ to globally align with the semantic content of both the target image $\boldsymbol{G}_{img}$ and the target text $\boldsymbol{p}^\star$, global features of $\boldsymbol{x'}, \boldsymbol{G}_{img}$ and $\boldsymbol{p}^\star$ are extracted by f_e and f_t. The global objective $\mathcal{M}_{global}$ is defined as:

$$\mathcal{M}_{global} = \mathrm{Cos}(f_e(\boldsymbol{x}'), f_e(\boldsymbol{G}^i_{img})) + \mathrm{Cos}(f_e(\boldsymbol{x}'), f_t(\boldsymbol{p}^\star_i)). \tag{11}$$

To further inject fine-grained semantics, we additionally align token-level features with $\boldsymbol{G}_{img}$. Let $f^{loc}_e(\cdot) \in \mathbb{R}^{m\times d}$ denote the local features of m image patch tokens, and d be the feature dimension of each token. The local similarity can be represented as:

$$\mathcal{M}_{local} = mean(\mathrm{Cos}(f^{loc}_e(\boldsymbol{x}'), f^{loc}_e(\boldsymbol{G}^i_{img})). \tag{12}$$

Finally, the overall alignment objective $\mathcal{M}_{src}$ can be calculated by:

$$\mathcal{M}_{src} = \mathcal{M}_{global} + \mathcal{M}_{local} \tag{13}$$

The adversarial perturbations $\boldsymbol{\delta}$ of the source image are updated to maximize $\mathcal{M}_{src}$ by:

$$\boldsymbol{\delta}^i = Clip_{\mathcal{B}_\epsilon}\{\boldsymbol{\delta}^{i-1} + \alpha_{src} \cdot sign\left(\nabla_{\boldsymbol{\delta}}\mathcal{M}_{src}\right)\}, \tag{14}$$

where α_{src} is the step size.

4. Experiments

4.1. Experimental Setup

Evaluated models and tasks: We primarily evaluate the effectiveness of the proposed adversarial prompt injection attacks on SOTA commercial MLLMs, including GPT-4o, GPT-5, Claude-4.5 and Gemini-2.5, under a black-box threat model. In this setting, the attacker has no access to model parameters, gradients, or internal states. To further assess the generalization capability of the proposed attack, we conduct evaluations across two downstream multimodal tasks, including:

- **Image Captioning:** Following the experimental protocols in (Li et al., 2025; Jia et al., 2025), we sample

Table 1. Performance under the soft criterion (target-image caption) on the image captioning task against different closed-source MLLMs.

Method	Surrogate	GPT-4o		GPT-5		Gemini-2.5		Claude-4.5	
		ASR↑	AvgSim↑	ASR↑	AvgSim↑	ASR↑	AvgSim↑	ASR↑	AvgSim↑
AttackVLM	B/16	0%	0.002	0%	0.0	0%	0.0	0%	0.0
	B/32	1%	0.005	0%	0.002	0%	0.002	0%	0.0
	Laion	0%	0.002	0%	0.002	0%	002	0%	0.002
AnyAttack	Ensemble	0%	0.012	0%	0.002	2%	0.01	0%	0.002
M-Attack	Ensemble	43%	0.199	32%	0.140	71%	0.281	3%	0.019
FOA-Attack	Ensemble	47%	0.232	27%	0.128	71%	0.291	6%	0.024
Agent-Attack	Ensemble	10%	0.058	10%	0.049	7%	0.039	0%	0.01
ours	Ensemble	**81%**	**0.442**	**56%**	**0.320**	**79%**	**0.429**	**8%**	**0.046**

Table 2. Performance under the hard criterion (target text) on the image captioning task against different closed-source MLLMs.

Method	Surrogate	GPT-4o		GPT-5		Gemini-2.5		Claude-4.5	
		ASR↑	AvgSim↑	ASR↑	AvgSim↑	ASR↑	AvgSim↑	ASR↑	AvgSim↑
AttackVLM	B/16	0%	0.0	0%	0.0	0%	0.0	0%	0.0
	B/32	0%	0.0	0%	0.0	0%	0.0	0%	0.0
	Laion	0%	0.0	0%	0.0	0%	0.0	0%	0.0
AnyAttack	Ensemble	0%	0.0	0%	0.0	0%	0	0%	0.004
M-Attack	Ensemble	32%	0.121	29%	0.105	65%	0.223	6%	0.026
FOA-Attack	Ensemble	42%	0.17	22%	0.099	69%	0.239	3%	0.013
Agent-Attack	Ensemble	3%	0.017	7%	0.033	4%	0.02	0%	0.0
ours	Ensemble	**74%**	**0.339**	**53%**	**0.249**	**81%**	**0.348**	**7%**	**0.029**

100 images from the NIPS 2017 Adversarial Attacks and Defenses Competition dataset and task the models with generating descriptive captions for each image.

- **Visual Question Answering (VQA):** We evaluate the attack on 100 image–question pairs randomly selected from the ScienceQA dataset (Lu et al., 2022), covering a wide range of visual reasoning scenarios.

Compared methods. We comprehensively compare the proposed method with two SOTA adversarial attack baselines, M-Attack (Li et al., 2025) and FOA (Jia et al., 2025), which are specifically designed to attack commercial MLLMs. AnyAttack (Zhang et al., 2025) is a self-supervised framework that generates targeted adversarial sample using a trained noise generator. AttackVLM (Zhao et al., 2023) also employs matching image-text features and image-image features, where its target image is generated from text by Stable Diffusion (Rombach et al., 2022). As these methods are originally tailored for the image captioning task rather than malicious prompt injection, we adapt them to our threat setting to enable a fair comparison. Specifically, we designate our base visual ground truth $\boldsymbol{G}^0_{img}$ embedded with explicit textual prompts as the adversarial target, ensuring that the injected instructions are visually aligned with the target commands required by our method. This adaptation allows all compared approaches to operate under a unified attack objective. We also compare our method with Agent-Attack (Wu et al., 2024), which attacks an image through matching image-to-text features.

Implementation details: We follow the experimental setup of M-Attack (Li et al., 2025) to deploy our method, in which CLIP-B/16 (Radford et al., 2021), CLIP-B/32 (Radford et al., 2021), and LAION (Schuhmann et al., 2022) are employed as surrogate feature extractors for gradient-based optimization. The optimization epochs is set to 300. Constraint ϵ is set to 16 for both source images and target images. α_{src}, α_{tgt}, λ_{pull} and λ_{push} are set to 1, 1, 1 and 0.5. To ensure the imperceptibility of the injected perturbations, we constrain the overall input modification, comprising both the covert trigger and the adversarial perturbation, within an ℓ_∞ norm bound of $\varepsilon = 16$. To evaluate the command expressivity of the proposed method, we consider two categories of malicious target commands that span varying levels of semantic complexity and potential real-world impact. Specifically, we design the following adversarial objectives:

- **Misinformation**: For the VQA task, the MLLM is coerced into producing a predefined incorrect or mislead-

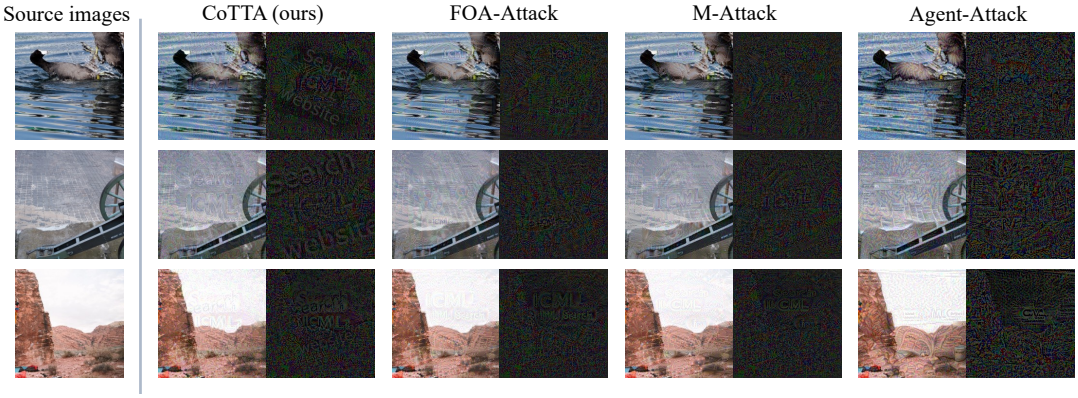

Figure 3. Visualization of adversarial examples and corresponding perturbations generated by different attacks.

Table 3. Performance under the hard criterion (target text) on the VQA task against different closed-source MLLMs.

Method	Surrogate	GPT-4o		GPT-5		Gemini-2.5		Claude-4.5	
		ASR↑	AvgSim↑	ASR↑	AvgSim↑	ASR↑	AvgSim↑	ASR↑	AvgSim↑
AttackVLM	B/16	0%	0	0%	0.000	1.00%	0.090	0%	0.000
	B/32	0%	0	0%	0.000	3.00%	0.022	0%	0.000
	Laion	0%	0	0%	0.000	0%	0.000	0%	0.000
AnyAttack	Ensemble	1%	0.003	0%	0.000	2%	0.008	0%	0.000
M-Attack	Ensemble	49%	0.442	11%	0.110	39%	0.380	0%	0.000
FOA-Attack	Ensemble	53%	0.492	12%	0.119	42%	0.418	0%	0.000
Agent-Attack	Ensemble	2%	0.017	0%	0.000	2%	0.010	0%	0.000
ours	Ensemble	**82%**	**0.820**	**58%**	**0.576**	**79%**	**0.787**	**2%**	**0.020**

ing response, such as "None of the above", regardless of the input question.

- **Action-Inducing Recommendations**: For the image captioning task, the MLLM is manipulated to generate persuasive or directive instructions that influence subsequent user decisions, for example, "Search ICML."

Evaluation metrics. For image captioning task, we adopt two complementary success criteria to reflect different levels of output control. The **soft** criterion treats the caption of the target text image as the reference, such as *"The image displays the text "Search ICML website" on a black background."*. The **hard** criterion requires the model to output the exact target sentence, assessing strict token-level controllability. For example, the ground truth text of hard criterion can be *"Search ICML website."*. For VQA task, we only assess hard criterion.

Following (Jia et al., 2025), we also utilize the LLM-as-a-judge framework. For the soft criterion, we use the same victim model to generate captions for both the target text image and the adversarial example, and then ask an LLM to judge the semantic similarity between the two captions. For the hard criterion, LLM judges the semantic similarity between the target text and the attacked output. If the similarity score exceeds 0.3, the attack is considered successful. The attack success rate (ASR) and the average similarity score (AvgSim) are reported.

4.2. Main Results

Comparisons in image captioning task. We evaluate multiple attacks on an image captioning task using four widely used closed-source MLLMs. The results of our CoTTA and other competitive methods are shown in Tables 1 and 2. From the results, it is evident that classic baselines such as AttackVLM and AnyAttack are largely unable to mislead the model into generating the target sentence. Our method substantially outperforms other methods, especially on the GPT-family models. Our attack achieves 81% and 74% ASR on GPT-4o under the soft and hard criteria, respectively, and outperforms the runner-up FOA-Attack by 31.5% ASR and 0.18 AvgSim on average across the GPT-family models. Beyond the GPT models, Gemini-2.5 also exhibits a pronounced vulnerability to our attack, achieving 79% and 81% success rates under the soft and hard criteria, respectively. Although FOA-Attack and M-Attack both at-

Table 4. Comparative results on 1000 images.

Method	Surrogate	GPT-4o		GPT-5		Gemini-2.5	
		ASR↑	AvgSim↑	ASR↑	AvgSim↑	ASR↑	AvgSim↑
FOA-Attack	Ensemble	41.3%	0.161	22.8%	0.089	58.4%	0.211
ours	Ensemble	64.7%	0.315	54.4%	0.246	73.2%	0.308

Table 5. Ablation studies of our proposed CoTTA.

Attacks	Soft		Hard	
	ASR↑	AvgSim↑	ASR↑	AvgSim↑
w/o covert trigger	66%	0.306	54%	0.202
w/o image-to-text alignment	75%	0.42	70%	0.348
w/o image-to-image alignment	27%	0.155	22%	0.081
w/o updating target image	73%	0.434	68%	0.351
CoTTA	81%	0.442	74%	0.339

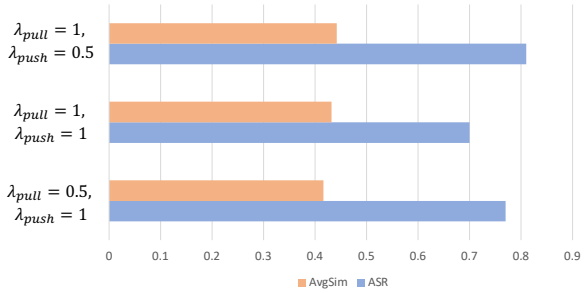

Figure 4. Ablation on weight coefficients $\lambda_{pull}, \lambda_{push}$.

tain reasonably strong ASR of 71% under the soft criterion, our AvgSim improves by 0.138 and 0.148 over them, respectively, indicating stronger overall alignment with the target beyond the binary success threshold. Claude-4.5 is the most robust model in our evaluation. All attacks show limited effectiveness, yet our method still achieves the highest ASR and AvgSim.

Figure 3 displays the adversarial images and their added modification resulting from our method and other competitive attacks. In the visualization, the perturbation of our method reveals an adaptive covert trigger pattern. Despite introducing a textual overlay, the resulting modifications remain visually subtle and natural, making them difficult to notice.

Comparisons in VQA task. We further evaluate all attacks on a VQA task, where the model answers questions grounded in the input image. Compared with captioning, VQA typically demands more fine-grained visual reasoning and question-conditioned attention over relevant regions. In this setting, our adversarial objective is to induce misinformation *"None of above."*. Performances are presented in Table 3. Our CoTTA significantly surpasses existing methods. Notably, it achieves AvgSim scores of 0.820 on GPT-4o and 0.787 on Gemini-2.5, with corresponding ASRs of 82% and 79%, respectively. Such high average similarities indicate that the generated outputs are consistently closer to the target sentence. On GPT-5, our method exceeds FOA-Attack by 46% in ASR and 0.457 in AvgSim.

4.3. Ablation Studies and Additional Experiments

We perform ablation studies on GPT4o to unravel the contributions our framework. Our method is decomposed into four components: covert trigger, image-to-text feature alignment, image-to-image feature alignment, and target-image updating. We ablate each by removing it in turn while keeping all other settings unchanged. As shown in Table 5, removing the image-to-image feature alignment causes the largest performance drop, reducing the ASR by 54% under the soft criterion and 52% under the hard criterion. The covert trigger leads to a 15% decrease in soft ASR when removed. The other two components also contribute noticeably to the overall performance. Combining all of the components yields the best results.

Results on 1000 images. To improve statistical reliability, we scale the evaluation to 1,000 samples and compare our method with the most competitive baseline, FOA-Attack, under the hard criterion. Table 4 summarizes the results, showing that our method outperforms FOA-Attack by a large margin, confirming the effectiveness of our method. Averaged over the three models, our method surpasses FOA-Attack by 23.27% in ASR and 0.136 in AvgSim.

Hyperparameter study of weights λ_{pull} and λ_{push}. We vary the two loss-weight coefficients and report ASR and AvgSim on GPT-4o in the image captioning task. As shown in Figure 4, setting $\lambda_{pull} = 1$ and $\lambda_{push} = 0.5$ delivers the best result.

5. Conclusion

In this work, we present CoTTA, a novel adversarial prompt injection framework that reliably induces targeted malicious outputs from closed-source MLLMs under a strict perturbation budget, especially when the malicious text cannot be naturally represented by a real-world image. CoTTA integrates an adaptive covert trigger with a perturbation that is jointly optimized through image-to-text and image-to-image alignment, and further strengthens attack consistency

and transferability via target-image updating. Specifically, we iteratively optimize the target image by adding perturbations to move its features closer to the target text while pushing them away from the attacked image. Extensive evaluations on image captioning and VQA demonstrate that CoTTA consistently exceeds existing methods across popular closed-source models. These results expose substantial vulnerabilities in modern MLLMs, and we hope CoTTA inspires future research toward more stealthy attacks and more precise, controllable adversarial manipulation.

Impact Statement

This work highlights previously underexplored security risks in multimodal large language models via an imperceptible adversarial prompt injection attack. By revealing such vulnerabilities, our findings aim to raise awareness and encourage the development of more robust defenses, detection mechanisms, and safety policies for MLLMs' deployment. We hope this work contributes to improving the reliability and responsible use of multimodal AI systems in safety-critical applications. Beyond these considerations, there are other potential societal consequences of our work, none of which we feel must be specifically highlighted here.

References

Achiam, J., Adler, S., Agarwal, S., Ahmad, L., Akkaya, I., Aleman, F. L., Almeida, D., Altenschmidt, J., Altman, S., Anadkat, S., et al. Gpt-4 technical report. *arXiv preprint arXiv:2303.08774*, 2023.

Agashe, S., Han, J., Gan, S., Yang, J., Li, A., and Wang, X. E. Agent s: An open agentic framework that uses computers like a human. *arXiv preprint arXiv:2410.08164*, 2024.

Bailey, L., Ong, E., Russell, S., and Emmons, S. Image hijacks: Adversarial images can control generative models at runtime. *arXiv preprint arXiv:2309.00236*, 2023.

Bucciarelli, D., Moratelli, N., Cornia, M., Baraldi, L., and Cucchiara, R. Personalizing multimodal large language models for image captioning: an experimental analysis. In *European Conference on Computer Vision*, pp. 351–368, 2024.

Cheng, H., Xiao, E., Wang, Y., Zhang, L., Zhang, Q., Cao, J., Xu, K., Sun, M., Hao, X., Gu, J., et al. Exploring typographic visual prompts injection threats in cross-modality generation models. *arXiv preprint arXiv:2503.11519*, 2025.

Clusmann, J., Ferber, D., Wiest, I. C., Schneider, C. V., Brinker, T. J., Foersch, S., Truhn, D., and Kather, J. N. Prompt injection attacks on vision language models in oncology. *Nature Communications*, pp. 1239, 2025.

Cohen, J., Rosenfeld, E., and Kolter, Z. Certified adversarial robustness via randomized smoothing. In *ICML*, 2019.

Cui, X., Aparcedo, A., Jang, Y. K., and Lim, S.-N. On the robustness of large multimodal models against image adversarial attacks. In *Proceedings of the IEEE/CVF Conference on Computer Vision and Pattern Recognition*, 2024.

Fang, W., Wu, Q., Chen, J., and Xue, Y. guided mllm reasoning: Enhancing mllm with knowledge and visual notes for visual question answering. In *Proceedings of the Computer Vision and Pattern Recognition Conference*, pp. 19597–19607, 2025.

Goodfellow, I. J., Shlens, J., and Szegedy, C. Explaining and harnessing adversarial examples. *arXiv preprint arXiv:1412.6572*, 2014.

Hein, M. and Andriushchenko, M. Formal guarantees on the robustness of a classifier against adversarial manipulation. *Advances in neural information processing systems*, 2017.

Jacob, D., Alzahrani, H., Hu, Z., Alomair, B., and Wagner, D. Promptshield: Deployable detection for prompt injection attacks. In *Proceedings of the Fifteenth ACM Conference on Data and Application Security and Privacy*, pp. 341–352, 2024.

Jia, X., Gao, S., Qin, S., Pang, T., Du, C., Huang, Y., Li, X., Li, Y., Li, B., and Liu, Y. Adversarial attacks against closed-source MLLMs via feature optimal alignment. In *The Thirty-ninth Annual Conference on Neural Information Processing Systems*, 2025.

Kimura, S., Tanaka, R., Miyawaki, S., Suzuki, J., and Sakaguchi, K. Empirical analysis of large vision-language models against goal hijacking via visual prompt injection. *arXiv preprint arXiv:2408.03554*, 2024.

Kuang, J., Shen, Y., Xie, J., Luo, H., Xu, Z., Li, R., Li, Y., Cheng, X., Lin, X., and Han, Y. Natural language understanding and inference with mllm in visual question answering: A survey. *ACM Computing Surveys*, pp. 1–36, 2025.

Kurakin, A., Goodfellow, I. J., and Bengio, S. Adversarial examples in the physical world. In *Artificial intelligence safety and security*, pp. 99–112. Chapman and Hall/CRC, 2018.

Li, J., Li, D., Savarese, S., and Hoi, S. Blip-2: Bootstrapping language-image pre-training with frozen image encoders and large language models. In *ICML*, 2023.

Li, W., Fan, H., Wong, Y., Yang, Y., and Kankanhalli, M. Improving context understanding in multimodal large language models via multimodal composition learning. In

Forty-first International Conference on Machine Learning, 2024a.

Li, X., Zhang, M., Geng, Y., Geng, H., Long, Y., Shen, Y., Zhang, R., Liu, J., and Dong, H. Manipllm: Embodied multimodal large language model for object-centric robotic manipulation. In *Proceedings of the IEEE/CVF Conference on Computer Vision and Pattern Recognition*, pp. 18061–18070, 2024b.

Li, Z., Peng, B., He, P., and Yan, X. Evaluating the instruction-following robustness of large language models to prompt injection. In *Proceedings of the 2024 conference on empirical methods in natural language processing*, pp. 557–568, 2024c.

Li, Z., Zhao, X., Wu, D.-D., Cui, J., and Shen, Z. A frustratingly simple yet highly effective attack baseline: Over 90% success rate against the strong black-box models of gpt-4.5/4o/o1. In *ICML 2025 Workshop on Reliable and Responsible Foundation Models*, 2025.

Lin, H., Lao, Y., Geng, T., Yu, T., and Zhao, W. Uniguardian: A unified defense for detecting prompt injection, backdoor attacks and adversarial attacks in large language models. *arXiv preprint arXiv:2502.13141*, 2025.

Liu, H., Li, C., Wu, Q., and Lee, Y. J. Visual instruction tuning. *Advances in neural information processing systems*, pp. 34892–34916, 2023a.

Liu, X., Zhu, Y., Lan, Y., Yang, C., and Qiao, Y. Safety of multimodal large language models on images and texts. *arXiv preprint arXiv:2402.00357*, 2024a.

Liu, Y., Deng, G., Li, Y., Wang, K., Wang, Z., Wang, X., Zhang, T., Liu, Y., Wang, H., Zheng, Y., et al. Prompt injection attack against llm-integrated applications. *arXiv preprint arXiv:2306.05499*, 2023b.

Liu, Y., Jia, Y., Geng, R., Jia, J., and Gong, N. Z. Formalizing and benchmarking prompt injection attacks and defenses. In *33rd USENIX Security Symposium (USENIX Security 24)*, pp. 1831–1847, 2024b.

Lu, P., Mishra, S., Xia, T., Qiu, L., Chang, K.-W., Zhu, S.-C., Tafjord, O., Clark, P., and Kalyan, A. Learn to explain: Multimodal reasoning via thought chains for science question answering. *Advances in neural information processing systems*, 2022.

Lu, W., Zeng, Z., Zhang, K., Li, H., Zhuang, H., Wang, R., Chen, C., and Peng, H. Argus: Defending against multimodal indirect prompt injection via steering instruction-following behavior. *arXiv preprint arXiv:2512.05745*, 2025.

Pathade, C. Invisible injections: Exploiting vision-language models through steganographic prompt embedding. *arXiv preprint arXiv:2507.22304*, 2025.

Qi, X., Huang, K., Panda, A., Henderson, P., Wang, M., and Mittal, P. Visual adversarial examples jailbreak aligned large language models. In *AAAI*, 2024.

Radford, A., Kim, J. W., Hallacy, C., Ramesh, A., Goh, G., Agarwal, S., Sastry, G., Askell, A., Mishkin, P., Clark, J., et al. Learning transferable visual models from natural language supervision. In *ICML*, 2021.

Rombach, R., Blattmann, A., Lorenz, D., Esser, P., and Ommer, B. High-resolution image synthesis with latent diffusion models. In *Proceedings of the IEEE/CVF conference on computer vision and pattern recognition*, pp. 10684–10695, 2022.

Schaeffer, R., Miranda, B., and Koyejo, S. Are emergent abilities of large language models a mirage? In Oh, A., Naumann, T., Globerson, A., Saenko, K., Hardt, M., and Levine, S. (eds.), *Advances in Neural Information Processing Systems*, pp. 55565–55581, 2023.

Schuhmann, C., Beaumont, R., Vencu, R., Gordon, C., Wightman, R., Cherti, M., Coombes, T., Katta, A., Mullis, C., Wortsman, M., et al. Laion-5b: An open large-scale dataset for training next generation image-text models. *Advances in neural information processing systems*, pp. 25278–25294, 2022.

Shi, J., Yuan, Z., Liu, Y., Huang, Y., Zhou, P., Sun, L., and Gong, N. Z. Optimization-based prompt injection attack to llm-as-a-judge. In *Proceedings of the 2024 on ACM SIGSAC Conference on Computer and Communications Security*, pp. 660–674, 2024.

Team, G., Georgiev, P., Lei, V. I., Burnell, R., Bai, L., Gulati, A., Tanzer, G., Vincent, D., Pan, Z., Wang, S., et al. Gemini 1.5: Unlocking multimodal understanding across millions of tokens of context. *arXiv preprint arXiv:2403.05530*, 2024.

Vaswani, A., Shazeer, N., Parmar, N., Uszkoreit, J., Jones, L., Gomez, A. N., Kaiser, Ł., and Polosukhin, I. Attention is all you need. *Advances in neural information processing systems*, 30, 2017.

Wang, L., Ying, Z., Zhang, T., Liang, S., Hu, S., Zhang, M., Liu, A., and Liu, X. Manipulating multimodal agents via cross-modal prompt injection. In *Proceedings of the 33rd ACM International Conference on Multimedia*, pp. 10955–10964, 2025.

Wang, Y., Liu, C., Qu, Y., Cao, H., Jiang, D., and Xu, L. Break the visual perception: Adversarial attacks targeting encoded visual tokens of large vision-language models. In *ACM MM*, 2024.

Webb, T., Holyoak, K. J., and Lu, H. Emergent analogical reasoning in large language models. *Nature Human Behaviour*, pp. 1526–1541, 2023.

Wei, J., Tay, Y., Bommasani, R., Raffel, C., Zoph, B., Borgeaud, S., Yogatama, D., Bosma, M., Zhou, D., Metzler, D., et al. Emergent abilities of large language models. *arXiv preprint arXiv:2206.07682*, 2022.

Wu, C. H., Shah, R., Koh, J. Y., Salakhutdinov, R., Fried, D., and Raghunathan, A. Dissecting adversarial robustness of multimodal lm agents. *arXiv preprint arXiv:2406.12814*, 2024.

Xia, S., Yu, Y., Jiang, X., and Ding, H. Mitigating the curse of dimensionality for certified robustness via dual randomized smoothing. In *The International Conference on Learning Representations*, 2024.

Xie, P., Bie, Y., Mao, J., Song, Y., Wang, Y., Chen, H., and Chen, K. Chain of attack: On the robustness of vision-language models against transfer-based adversarial attacks. In *Proceedings of the IEEE/CVF Conference on Computer Vision and Pattern Recognition*, 2025.

Yi, J., Xie, Y., Zhu, B., Kiciman, E., Sun, G., Xie, X., and Wu, F. Benchmarking and defending against indirect prompt injection attacks on large language models. In *Proceedings of the 31st ACM SIGKDD Conference on Knowledge Discovery and Data Mining V. 1*, pp. 1809–1820, 2025.

Zhang, J., Ye, J., Ma, X., Li, Y., Yang, Y., Chen, Y., Sang, J., and Yeung, D.-Y. Anyattack: Towards large-scale self-supervised adversarial attacks on vision-language models. In *Proceedings of the Computer Vision and Pattern Recognition Conference*, pp. 19900–19909, 2025.

Zhao, Y., Pang, T., Du, C., Yang, X., Li, C., Cheung, N.-M. M., and Lin, M. On evaluating adversarial robustness of large vision-language models. *Advances in Neural Information Processing Systems*, pp. 54111–54138, 2023.

Zheng, B., Gou, B., Kil, J., Sun, H., and Su, Y. Gpt-4v (ision) is a generalist web agent, if grounded. *arXiv preprint arXiv:2401.01614*, 2024.